Paper ID:77

A Study on Enhanced Thermal Performance in Two-Phase Microchannels for Electronic Cooling Applications

Md Nadimul Akram[1], Md Al Shahriar Akash[2], Mohammed Harunur Rashid[3]

[1]School of Energy and Environment, Southeast University, Nanjing, 210096, PR China
E-mail: nadim.akram684679@gmail.com
[2]School of Integrated Circuit, Southeast University, Nanjing, 210096, PR China
E-mail: akashalshahriar@gmail.com
[3]School of Electrical Engineering, Southeast University, Nanjing, 210096, PR China
E-mail: mohammedharunur64@gmail.com

Abstract

Two-phase microchannel heat sinks are in great demand across industries such as microelectronics, defense, energy, solar, and medical components. This is because they have efficient heat transfer capabilities, a compact size, and a high heat transfer coefficient (HTC). However, challenges such as large wall superheat, flow instability, and low critical heat flux in conventional solid parallel microchannels have limited their practical applications for high heat flux dissipation. Dielectric fluids are difficult to use for promoting critical heat flux (CHF) without precooling due to their high vapor density, low surface tension, and excellent wettability. In recent years, significant efforts have been made to address these challenges by designing and fabricating enhanced microchannels for flow boiling in two-phase microchannel heat sinks. This study thoroughly examines recent advancements in flow boiling enhancement microchannels, with a specific focus on its application in electronic cooling and a focus on super-capillary pin-fin fences. The paper discusses the performance of these enhanced microchannels in flow boiling enhancement and cooling techniques and concludes by outlining the challenges and future research directions in this area.

Keywords: Enhanced microchannels, Flow boiling**,** Micro-nozzles, CHF, Nanostructure

1. Introduction

Effective cooling solutions become critical as high-power electronic devices continue to shrink to nanometer sizes. Flow boiling in microchannels is one of the most effective methods for cooling these devices due to its high cooling capabilities [1]. However, enhancing boiling heat transfer in microchannels without performance compromises remains challenging, primarily due to confined vapor bubbles that limit the system's effectiveness. Achieving higher critical heat flux (CHF) values is crucial to increase the safety margin in nuclear power plants' systems like two-phase heat exchangers and thermal-hydraulic systems. With increasing power density and miniaturization of electronic components, the demands for effective cooling have risen dramatically [2]. Compared to single-phase cooling methods, two-phase cooling in closed microchannels offers significant advantages in packaging and enhanced thermal performance, making it one of the most promising solutions for high-power electronic cooling [3]. By employing phase change, these systems leverage the coolant’s latent heat rather than its sensible heat, achieving much greater heat transfer coefficients. However, with growing speed and functionality in electronics and continued size reductions, heat dissipation requirements are increasing exponentially [4]. Nevertheless, two-phase flow instabilities pose serious challenges. They can cause reverse flows, resulting in liquid supply crises and compromising performance [5]. The bubble confinement effect in closed microchannels, a well-known phenomenon, makes it more difficult to regulate two-phase flows compared to regular-sized systems. Although there has been significant progress, conflicting trade-offs in performance remain due to the stochastic nature and transitional boundary layer dynamics of two-phase flow. One critical challenge is liquid supply shortages at the microchannel outlet, which limits overall performance [6]. Our recent studies indicate that microchannel configurations with multiple micronozzles

and internal re-entrants (IRs) Show promise in enhancing liquid distribution throughout the channel. Our earlier work utilized a microfluidic transistor to induce high-frequency self-sustained two-phase oscillations (TPOs), achieving desirable two-phase mixing without needing external controllers or additional pressure sources [7]. However, the presence of only a single pair of nozzles in the middle of each main channel led to constricted vapor slugs upstream, limiting the mixing range. The limited nucleation sites also hindered efforts to improve the flow boiling heat transfer rate [8]. Therefore, this review aims to summarize recent advancements in heat transfer enhancement techniques for flow boiling in microchannels and to identify research gaps and objectives for further progress in this field.

2. Design and experimental procedures

This section provides a detailed discussion of the design principles of the test chip. The new configuration was developed based on prior research involving microneedle fences and multiple micronozzles to enhance system performance. Our focus is on explaining the design concept and conducting an in-depth analysis of the experimental process and the measurement methods employed. By comparing the experimental data from different design solutions, we verify the effectiveness of the new configuration in improving performance. These experimental results offer a theoretical foundation for further optimization and pave the way for future applications.

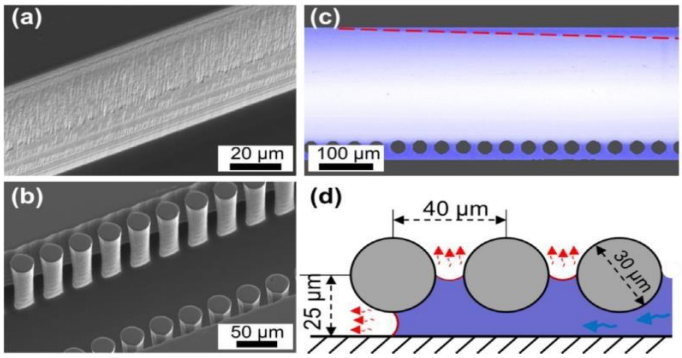


Fig. 1. Development of conceptualization. (a) The SEM image of a plain wall, (b) an SEM image of micropinfin fences, (c) the top-view of the receding liquid profile on the smooth wall and the one on the wall with micro-pin fin fences (re-colored image, blue represents liquid of water) and, (d) schematic of the thin film evaporation within micro-pin fin fence[9]. Note: (Li, W., et al., *Enhanced flow boiling in microchannels integrated with super capillary pin fin fences.* International Journal of Heat and Mass Transfer, 2022. **183**: p. 122185)

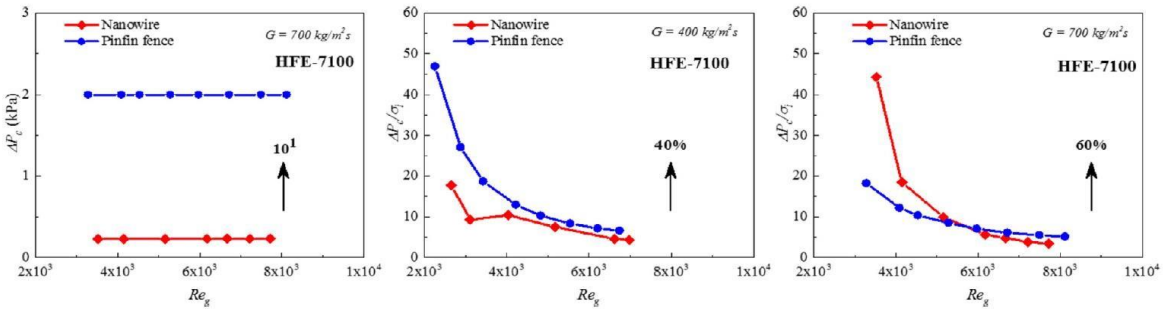


Fig. 2. (a) capillary pressure comparison, (b, c) ratio of capillary pressure over interfacial stress for various mass fluxes on HFE-710[9] Note: (Li, W., et al., *Enhanced flow boiling in microchannels integrated with super capillary pin fin fences.* International Journal of Heat and Mass Transfer, 2022. **183**: p. 122185)

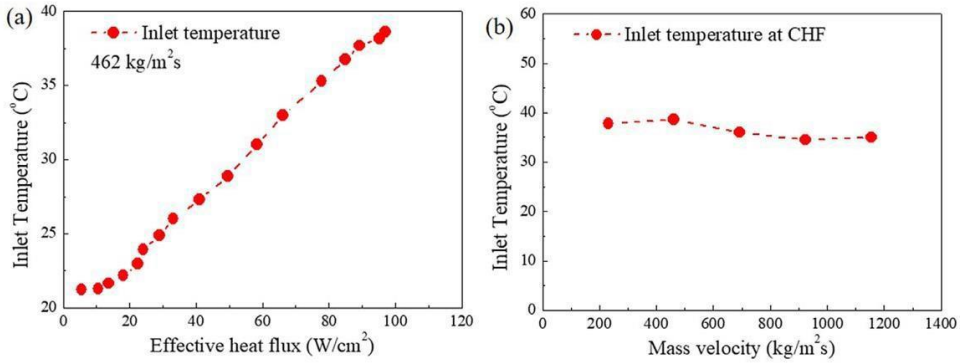


Fig. 3. (a-f) Thin film dynamics on both plain wall and micro-pin fin fence wall in one channel at working conditions of 90 W/cm^2 and G = 160 kg/m^2 s on water. The reddish line in (b) shows the dynamic liquidvapor interface on the plain wall[9]Note: (Li, W., et al., *Enhanced flow boiling in microchannels integrated with super capillary pin fin fences.* International Journal of Heat and Mass Transfer, 2022. **183**: p. 122185 Copyright 2022 by Li Wenming)

In a traditional microchannel with smooth sidewalls, a very thin liquid film can be momentarily generated on the sidewalls and channel corners after vapor slugs expand along the channel. To illustrate the difference in the thin liquid film profile, a microchannel was designed and fabricated with a smooth wall on one side and a micro-pin fin fence on the other side. A snapshot of the development of thin liquid film on both walls clearly shows the difference in terms of profile. On the smooth sidewall, the receding contact angle of the liquid front is about 5° (in Fig. 1c), much smaller than the advancing contact angle of about 40 ± 2°. Under high heat fluxes, the thin liquid film would quickly evaporate, leading to a dry-out crisis or premature CHF (Critical Heat Flux) conditions. However, capillary microarchitectures designed along each vertical wall inside microchannels can maintain a thin liquid film. During the boiling process, the liquid-vapor interface is established next to the micro-pinfin fence, and a uniform thin liquid film forms between the wall and the micro-pinfin fence. This film acts as a reconstructed two-phase boundary layer (BL) that results from the induced capillary action. This stable and sustainable thin liquid film can be regulated and controlled by adjusting the gap between the sidewall and micro-pin fin fence, as well as the pitch of the micro-pin fin. In this study, the micropillar is characterized with a diameter and height of 30 μm and 250 μm, respectively. More importantly, the enhanced capillary action plays a key role in maintaining the liquid film. To illustrate the rationale of the present design of the micro-pin fin fence in regulating two-phase flows, comparisons between capillary pressures in silicon nanowire (SiNW) microchannels and the micro-pin fin gap are shown. The interfacial stress on the vapor-liquid interface is calculated by σi = _P f D h 4L, where _P f is the frictional pressure drop. The equation _P c = 4 γcosθd n computes capillary pressure. Here, d n is the characteristic length scale. In this study, d n is the gap between the wall and micro-pinfin fence, about 10 μm. Hence, the capillary pressure induced by the gap is about 29 kPa at room temperature. On HFE-7100, the capillary pressure is about 10 times greater than that inside SiNW microchannels. Therefore, the micro-pin fin microchannel experiences continuous and uniform rewetting throughout the channel length. This indicates that capillary pressure is higher than interfacial stress in two different channels, which can sustain the thin liquid film and improve liquid renewal.

3. Data Reduction

The measured voltage, current, and pressure will calculate the boiling heat transfer.

Firstly, the total input power was determined by:

$$P = VI \tag{1}$$

The resistance of the micro-heater was calculated as:

$$R = V / I \tag{2}$$

The amount of heat dissipated through boiling was estimated by:

$$Q_{lantent} = P - Q_{loss} - Q_{sensible} \tag{3}$$

Where $Q_{sensible}$ is the sensible heat, component by:

$$Q_{sensible} = GA_c C_p (T_{out} - T_{in}) \tag{4}$$

The average bottom temperature of the micro-heater was then derived by:

$$T_{heater} = K.(R - R_a) + T_a \tag{5}$$

Where parameter m was estimated from

$$m = \sqrt{2h(L+W) / k_s WL} \tag{6}$$

Finally, the effective two-phase HTC was calculated by:

$$h_{tp} = \frac{Q_{lantent}}{(\sum (WL - 2HLf)(T_{wall} - T_{sat})} \tag{7}$$

Here, T_{sat} was calculated by referring to the middle pressure of the channel,

$$P = P_i - \frac{\Delta P}{2} \tag{8}$$

Additionally, exit vapor quality was calculated according to;

$$Q = \frac{P_{eff} - Q_{sensible}}{mh_{fg}} \tag{9}$$

4. Result and discussion

4.1 Incorporating multiple micro-nozzles and micro-pin fin fences

This section discusses the reasoning behind the tested chip's design. This innovative design is based on previous research on micro-pin fin fences and numerous micronozzles. The experimental methodologies and measurements are also discussed. The tested device was constructed from a silicon wafer attached to a Pyrex wafer using a typical microfabrication procedure described in our earlier paper. The functional features were created on a double-sided polished n-type 100> silicon wafer. A thin aluminum film heater (length: 10 mm, width: 2 mm, thickness: 1.2 m) was coated on the device's underside to imitate the heat flux. It also functions as a theorist to gauge the temperature of the wall. Following chip etching, a 500 m thick Pyrex glass wafer was glued to the silicon substrate to close the channels and produce a visualization window. DI-water and dielectric fluid HFE-7100 at room temperature were employed as working fluids in this investigation to analyze the flow boiling performance of the current design. Subcooled flow boiling in microchannels was investigated in this study. However, before entering the tested chip, the working fluids were heated by the testing stage, which was constructed of copper blocks. The inlet temperatures of coolants were measured to determine the proportion of sensible heat to total dissipated heat fluxes. For example, at a mass velocity of 462 kg/m2s, the inlet temperatures of the HFE-7100 were measured, as shown in Figure .3. Pte-calibration between the electric resistance of the micro-heater and the operating temperature was performed to measure the temperature of the micro-heater. Before testing, the thin film heater was calibrated in an isothermal oven. The temperature of the heater and its electrical resistance were found to be related. The linear fitting slope was used to estimate the surface temperatures of the tested device. The enhancement mechanism was mainly attributed to increased wettability in delaying CHF and nucleation sites formed by the nanowire bundles to improve the HTC in the nucleate boiling regime. However, the annular flow regime typically dominates at high heat fluxes, where film evaporation is the important heat transfer mode.

Enhanced CHFs Physical limits of flow boiling along with significant enhancements of CHF compared to SiNWs and plain wall were demonstrated. The micro-pin fin fence provides the capacity that allows for quick liquid replenishment, improves local liquid spreading, and mitigates dry-out crises. In contrast to pre-cooled coolant, the coolant of the HFE-7100 in this investigation was slightly heated by the copper block of the testing stage before entering the tested device. Figure 5a shows that the inlet temperature of the HFE-7100 grew from 20 ℃ to 39 ℃ as effective heat fluxes increased at a specific mass velocity of 462 kg/m2 s. Figure 5b depicts the inlet temperature of the HFE-7100, maintaining 37 ℃ near CHF conditions for various mass velocities. These near-CHF inlet temperatures can be used to calculate the contribution of sensible heat to overall dissipated heat fluxes (CHF values). The rise in intake temperatures also reflects a decrease in the contribution of sensible heat to CHF values. The phase change heat transfer dissipates more heat fluxes. The near-CHF inlet temperatures can be used to calculate the contribution of sensible heat to overall dissipated heat fluxes (CHF values). The rise in intake temperatures also reflects a decrease in the contribution of sensible heat to CHF values. The phase change heat transfer dissipates more heat fluxes. Flow boiling in the proposed SiNW-pin-fin microchannels has been experimentally characterized and compared with the plain wall, SiNWs decorated, and μ-pin-fin microchannels. All experiments are performed within a mass flux range of 231–1150 kg/(m2•s) and a heat flux range of zero to CHF conditions. The effect of flow pattern alternation incited by the SiNW-pin fin structure on the flow regimes of flow boiling is also explored via a visualization study.

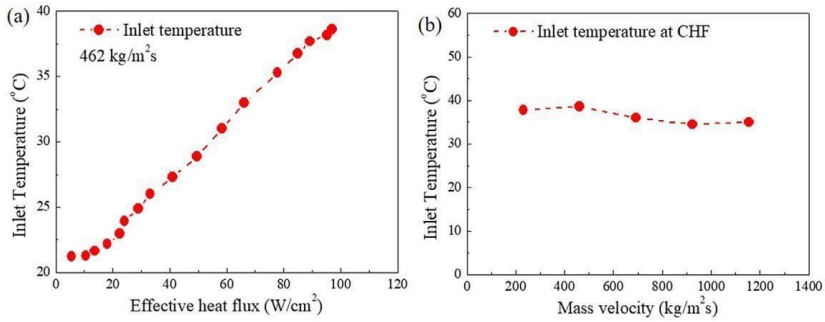


Figure 3. (a) The inlet temperature increases with the increasing of effective heat flux and (b) the inlet temperature is almost constant near CHF conditions on HFE-7100 [10, 11] (Note: Li, W., et al., *A remarkable CHF of 345W/cm2 is achieved in a wicked-microchannel using HFE-7100.* International Journal of Heat and Mass Transfer, 2022. **187**: p. 122527, copyright 2022 by Li Wenming)

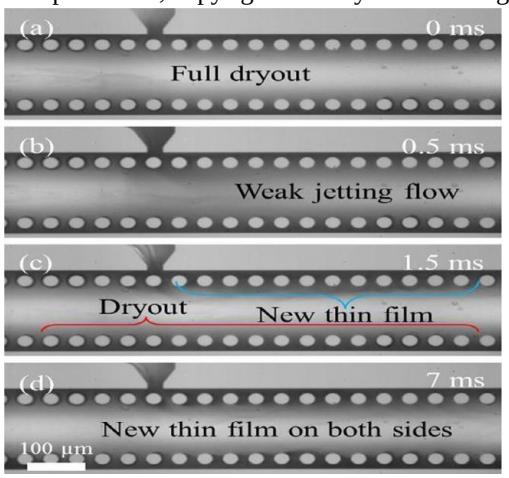


Figure 4. The decreased rewetting ability at CHF conditions near the third nozzle at a mass velocity of 231 kg/m2s: (a) full dry out was observed in the channel, (b) liquid was supplied to the channel through the jetting follow from the auxiliary channel, (c) the side wall of the channel was partially rewetted, and (d) both sides of the channel were rewetted[11](Note: Li, W., et al., *A remarkable CHF of 345W/cm2 is achieved in a wicked-microchannel using HFE-7100.* International Journal of Heat and Mass Transfer, 2022. **187**: p. 122527, copyright 2022 by Li Wenming)

5. Conclusion

This study provides a comprehensive analysis of recent advancements in flow boiling within improved microchannels. Generally, there are two main approaches to enhancing microchannels. The first involves modifying the walls or bottom surfaces of the microchannels. This can be achieved through techniques such as creating reentrant micro-cavities, adding porous layers, and incorporating nanostructures onto the walls or bottom surfaces of the microchannels. These methods are frequently capable of increasing heat transfer regions, increasing bubble nucleation sites, changing surface wettability, mitigating severe two-phase instability, or delaying the onset of CHF. The other option is to modify the flow passages with flow disruption structures (for example, micro pin fins or cross-linked microchannels), reentrant flow passages of microchannels, or porous-based microchannels. These approaches generally help improve flow distribution and redevelopment of thermal boundary layers, provide more passages for vapor flow, and modify the flow pattern. The two directions of enhanced microchannels promote the flow boiling enhancement in HTC, CHF, or two-phase flow instability. Nevertheless, four important issues should be addressed for the surface enhancement methods for their better practical applications. Based on comprehensive reviews of flow boiling enhancement in microchannels presented above, it is suggested that future research on enhanced microchannel flow boiling be concentrated on Hybrid enhanced microchannels with the integration of several enhancement structures are good choices to combine the merits for further flow boiling enhancement of microchannels heat sinks. Advanced microchannels for further flow boiling enhancement with or without a significant increase in pressure drop loss are favorable and attractive. Even though most enhancement methods allow for heat transfer and pressure drop increase, a trade-off must be made between heat transfer and pumping power. This should be explicitly compromised for the commercialization of enhanced microchannel heat sinks. Further study is needed to optimize key parameters for enhanced structures, such as shape, size, and layout of flow disruption structures, reentrant cavities, porous structures, and nanostructures.

Nomenclature

a	channel aspect ratio	c	surface tension, N/m
A	area, m²	h	contact angle
C_c	parameter for exit effect	ℓ	viscosity, kg/(s m)
C_f	frictional coefficient	q	density, kg/m³
D	diameter, m	v	vapor quality
H	height, m	r_i	interfacial stress, N/m²
h_{fg}	latent heat of vaporization, kJ/kg	s	flow area contraction ratio
f	fanning friction factor, m		
G	mass flux, kg/m² s	*Subscripts*	
k_d	momentum correction factor, W/m K	2/	two-phase
L	length, m	*acc*	accelerational
$m_$	mass flow rate, kg/s	*c*	cross section
N	number of pin fins	*CHF*	critical heat flux
Dp	pressure drop, Pa	*e*	exit
P	power, W	*eff*	effective
S	slip coefficient	*exp*	experimental
S_T	transverse pitch, m	*f*	frictional
u	velocity, m/s	*h*	hydraulic
u	average velocity, m/s	*i*	inlet
W	microchannel width, m	*l*	liquid
z	coordinate, m	*m*	mixture
		o	outlet

References

1. Lin, Y., et al., *Enhancement of flow boiling heat transfer in microchannel using micro-fin and microcavity surfaces.* International Journal of Heat and Mass Transfer, 2021. **179**: p. 121739.
2. Jiang, X., et al., *Design of micro-nano structures for counter flow diverging microchannel heat sink with extraordinarily high energy efficiency.* Applied Thermal Engineering, 2022. **209**: p. 118229.
3. Wang, C., et al., *Enhanced heat transfer study of microchannel heat sink with periodically arranged triangular cavities and arc-shaped ribs.* Heat Transfer, 2024. **53**(5): p. 2438-2459.
4. Ayatollahi, S., A. Ahmadpour, and M. Hajmohammadi, *Performance evaluation and optimization of flattened microchannel heat sinks for the electronic cooling application.* Journal of Thermal Analysis and Calorimetry, 2022. **147**(4): p. 3267-3281.
5. Ma, D.D., et al., *Experimental investigation of flow boiling heat transfer performance in zigzag microchannel heat sink for electronic cooling devices.* International Journal of Thermal Sciences, 2019. **145**: p. 106003.

6. Chang, W., et al., *Enhanced flow boiling in microchannels integrated with hierarchical structures of micro-pinfin fences and nanowires.* Langmuir, 2021. **37**(30): p. 8989-8996.
7. Harris, M., et al., *Overview of recent trends in microchannels for heat transfer and thermal management applications.* Chemical Engineering and Processing-Process Intensification, 2022. **181**: p. 109155.
8. Yang, F., et al., *Flow boiling phenomena in a single annular flow regime in microchannels (II): Reduced pressure drop and enhanced critical heat flux.* International Journal of Heat and Mass Transfer, 2014. **68**: p. 716-724.
9. Li, W., et al., *Enhanced flow boiling in microchannels integrated with supercapillary pinfin fences.* International Journal of Heat and Mass Transfer, 2022. **183**: p. 122185.
10. Li, W., et al., *A remarkable CHF of 345W/cm2 is achieved in a wicked-microchannel using HFE-7100.* International Journal of Heat and Mass Transfer, 2022. **187**: p. 122527.
11. Li, W., J. Ma, and C. Li, *Enhanced flow boiling in microchannels by incorporating multiple micronozzles and micro-pin fin fences.* International Journal of Heat and Mass Transfer, 2021. **165**: p. 120695.